

USING OF ACTIVATED CARBON DERIVED FROM AGRICULTURE WASTE COATING BY LAYERED DOUBLE HYDROXIDE FOR COPPER ADSORPTION

M. F. Al Juboury¹H. M. Abdul-Hameed²

Researcher

Assist. Prof.

¹Env. Eng. dept. University of Baghdad, &
Civil Eng. Dept. University of Kerbala, Iraq maad.farooq@uokerbala.edu.iq

²Env. Eng. dept. University of Baghdad, Iraq
hayderabdul_hameed@yahoo.com

ABSTRACT

Mg/Fe layered double hydroxides (LDH) as highly effective clay adsorbents coating activated carbon derived from agricultural waste (AW) were prepared by activation of date palm leaf base (LB) synthesized on Mg/Fe layered double hydroxides. FTIR, SEM and EDS were used to characterize the obtained adsorbent for the copper removal from aqueous solutions. The evaluation of adsorption performances was carried out at various metal concentrations, adsorbent dosage, contact time, and pH. The pseudo-second-order kinetic and the Langmuir isotherm model showed a good compliance with the experimental data, the result demonstrated that the improving adsorption capacity and fast rating adsorption for Cu²⁺ resulted from successful intercalation of date palm petiole activated carbon into LDH.

Keywords: heavy metals, adsorption, Mg/Fe layered double hydroxides, activated carbon and petioles.

حسين وعبد الحميد

مجلة العلوم الزراعية العراقية - 2019: 50(5): 1446-1454

استعمال الكربون النشط المصنوع من المخلفات الزراعيه عند طلائه بالهيدروكسيد متعدد الطبقات لامتزاز النحاس

حيدر محمد عبد الحميد²معد فاروق حسين¹

استاذ مساعد

باحث

¹قسم الهندسة المدنيه - جامعه كربلاء^{2,1}قسم الهندسه البيئيه - جامعه بغداد

المستخلص

ان عمليه تركيب وتغليف حبيبات من سعف النخيل بعد تحويلها الى الكربون النشط من خلال عمليه التنشيط , مع هيدروكسيد متعدد الطبقات من المغنسيوم والحديد يؤدي الى انتاج ممتاز ذو كفاءه عاليه لازاله عنصر النحاس من المحلول المائي الملوث. ان ماده المركبه المنتجه تم فحصها بواسطه تحليل الطيف بالاشعه تحت الحمراء, مطياف تشتت الطاقه و تحليل الصوره المجهرية بالاشعه السينيه وقد اكدت نتائج الفحوصات على نجاح عمليه التركيب. وبالنسبه لعمليه امتزاز النحاس فتمت دراسته تأثرها بعدد من المتغيرات (تراكيز مختلفه للملوث, اوزان مختلفه للماده المازة, اوقات مختلفه وقرانات مختلفه للأس الهيدروجيني). ان المعادله من الدرجه الثانيه تكون اكثر مطابقه عند تحليل البيانات الحركية وان موديل Langmuir يكون اكثر مطابقه عند تحليل البيانات ثابتة درجه الحراره. ان النتائج من التجارب المختبريه بينت ان عمليه ازاله النحاس باستعمال ماده المنتجه تدل على كفاءه عاليه وهذا يدل على نجاح عمليه تصنيع المنتج من المخلفات الزراعيه.

الكلمات المفتاحيه: المعادن الثقيله, الامتزاز, هيدروكسيد متعدد الطبقات, كربون نشط, عنق الورقه.

INTRODUCTION

Contaminants of high toxicity like pesticides, dyes, and heavy metals are considered for one of the major environmental issues (30,1,3). The main source of metal ions are wastes resulting from smelting, mining, battery manufacturing, and metal plating which contaminate water environment (21,31,4). In soil ecosystems and natural water, heavy metals, such as aluminium, manganese, cobalt, molybdenum, chromium, cadmium, silver, and copper, are mobile and toxic and because of this, they are considered to be priority contaminants (15,11). As they cannot be destroyed or degraded easily, they are regarded as persistent and stable environmental pollutants (19,12,17). Removing of heavy metals from an aqueous solution is needful to comply with environmental regulations, and for the sake of human health and safety (32,28,2). Thus, there has been an increase in demand for technologies that are sustainable in terms of economy, efficiency, energy, and environment such as adsorption (5). Anionic clays or hydrotalcite-like compounds, which are another names for LDHs, also for their unique properties and special structure, deserve considerable attention (26). For their acid-base buffering capacity, reconstruction reactions, ion exchange capacity, and an increase in surface area, LDHs were studied as sorbents briefly (27). Moreover, previous studies have shown the effective removal of Cu^{2+} from aqueous systems on LDHs under different experimental conditions (10). The chemical composition of LDHs is $([\text{M}_1^{2+} \text{M}_2^{3+} (\text{OH})_2]^{x+} (\text{A}^{n-})_{x/n-m} \cdot \text{H}_2\text{O})$, where A^{n-} is an anion with charge n , M_1^{2+} and M_2^{3+} represent the divalent and trivalent metals, respectively, and x is equal to $\text{M}_1^{3+}/(\text{M}_1^{3+} + \text{M}_2^{2+})$ (generally = 0.2–0.33) (8). Previous studies have reported the copper removal by adsorption onto organic anions malate and citrate directly coating with Mg/Al-LDH (33), Zn/Al-LDH intercalated with EDTA (ethylene diamine tetra acetic acid) (14), Mg/Fe-LDH loaded with magnetic (Fe_3O_4) carbon spheres (36), and so indicated the best ways of the copper removal from aqueous systems. Yet, the date palm leaf base (LB), which was collected from the waste

produced in agriculture, shows lower removal efficiency compared to the LB improved by chemical and physical modification processes like activation to produce AW (2). As a result, the pure LB adsorption capacity is lower in comparison with the modified LB (AW) removal capacity because of its increased surface area (19). So, the use of AW coating by Mg/Fe-LDH as a sorbent for copper has not been reported in previous studies. In this study, the copper removal from wastewater was examined by using Fe/Mg layered double hydroxides synthesized with activated carbon from date palm petiole (AW/Fe/Mg-LDH).

MATERIALS AND METHODS

Materials and adsorbent preparation

The natural date palm leaf base (LB) was collected from agriculture waste resulting in an area located in the middle of Iraq. In order to clean the LB from dirt particles, it was washed many times with distilled water and then dried in the sunlight. Later, the well dried LB was crushed and sieved by using 1.19 to 0.595 mm mesh size (Fig. 1). After this, it was activated in the furnace at the temperature of 350 °C, using N_2 and CO_2 for (2 h), respectively.



Figure 1. Leaf base date balm from natural to activated carbon

The reagents for analytical grade were Na_2CO_3 , $\text{FeCl}_3 \cdot 6\text{H}_2\text{O}$, $\text{Mg}(\text{NO}_3)_2 \cdot 6\text{H}_2\text{O}$, HCl , and NaOH . A $\text{Cu}(\text{NO}_3)_2$ (from s.d. Fin. Chemi., Mum., India) solution with the concentration of 1000 mg/L was prepared and kept at room temperature of 25 °C. By using 0.1 M HCl or 0.1 M NaOH , the prepared solution pH was set for every copper solution in the experiment. By co-precipitation method, layered double hydroxides were prepared at laboratory temperature. Various molar ratio (Mg/Fe) (1, 2, 3, 4) of $\text{Mg}(\text{NO}_3)_2 \cdot 6\text{H}_2\text{O}$ and $\text{FeCl}_3 \cdot 6\text{H}_2\text{O}$, as well as various petiole dosages (5/100, 10/100, 30/100, 50/100,

100/100 and 200/100 g) were contained in the 50 mL of the solution. After this, in order to achieve pH = 7 for the solution, Na₂CO₃ (0.2 Mol) and NaOH (2 Mol) were added and then stirred in (1 h). The produced particles were washed and filtered by using deionized water. The final product was achieved by drying for 24 h at 80 °C.

Sorption studies of batch mode

In order to find the equilibrium data and to assign the best conditions including adsorbent dosage, contact time, pollutants init. conc., and pH relating to the process of treatment, the batch experiments were calculated. A 50 ml of the copper solution was put in each flask (250 mL) from a series of conical flasks and thermostatic shaker bath was used for shaking them for (3 h). To achieve adjustment of the solution pH, 0.1 Mol of HCl or 0.1 Mol of NaOH were added. To achieve equilibrium of mixtures, they were shaken and filtrated by filter paper. By utilizing atomic absorption spectrophotometer flame (AAS), the metal concentration was calculated, which was still present in the mixtures after filtration. The batch experiments were examined at different parameters: various adsorbent dosage (0.02, 0.04, 0.06, 0.08, 0.1, 0.15, 0.2, and 0.3 g/50 mL), different values of initial concentration of contaminant (5, 10, 50, 100, 150, 200, 500, and 1000 mg/l), pH (3, 4, 5, and 6) and time (5, 10, 20, 30, 60, and 180 min). The value of (q_e), which represents the amount of pollutant adsorbed by the adsorbent, was calculated using the following formula (35).

$$q_e = (C_o - C_e) \frac{V}{m} \quad (1)$$

The adsorbent mass (g) equals to m, the solution volume (l) equals to V, and the equilibrium and initial contaminant concentrations in the flask (mg/l) represent the C_e and C_o, respectively.

RESULTS AND DISCUSSION

Sample characterization

Scanning electron micrography (SEM) images showed the characterization morphologies of the samples (LB, AW, AW/Mg/Fe-LDH and AW/Mg/Fe-LDH after adsorption of copper)

(Fig. 2). The pores of the LB and AW structures compacted regularly, and they had ends, sharp corners and coarse surfaces. The AW, according to its surface area and structure, was coated with Mg/Fe-LDH or some different coating material. After composition, the particle of AW/Mg/Fe-LDH had a well-defined, uniform and regular lamellar structure, and within the size ranging from 83.6 to 24.3 nm the Mg/Fe-LDH was coating the AW. As shown in Figure 2, when copper was adsorbed onto AW/Mg/Fe-LDH, on the surface of the adsorbent, several uniform hexagonal plates such as crystals aggregate. The (Fig. 2) shows an EDS spectrum of activated carbon, which contains a high amount of C, Fe, Mg, and O. This figure also shows an EDS spectrum of the AW/Mg/Fe-LDH presenting an increasing amount of Fe and Mg, and by co-precipitation method, the AW was successfully coated by Mg/Fe-LDH. It is possible to say that the adsorbent was efficient for the copper adsorption due to the increasing amount of copper on it. Fourier transform infrared (FTIR) spectra of LB, AW, AW/Mg/Fe-LDH, and AW/Mg/Fe-LDH after adsorption of copper are presented in (Fig. 3), where significantly less functional group types appear on the surface (Table 1). From the new peaks at 1369 cm⁻¹, a good modification of Mg/Fe-LDH on AW according to the asymmetric stretch absorption band of the CO₃⁻² is seen, and they are observed in AW/Mg/Fe-LDH composites (18). The carbonate has to exchange with copper which leads to a change of the bands after adsorption of copper (24). The band At 597 cm⁻¹ refers to the lattice vibrations of O-M-O and M-O (where M stands for metals). The band at 3387 cm⁻¹ represents the stretching vibration of (adsorbed water, O-H groups of adjacent layers, and interlamellar water), which bonded to hydroxyl groups (34). Vibrational modes of amide I and amide II proteins are represented by 1656 (C = O stretching) and 1552 (N-H deformation) peaks, respectively (24)

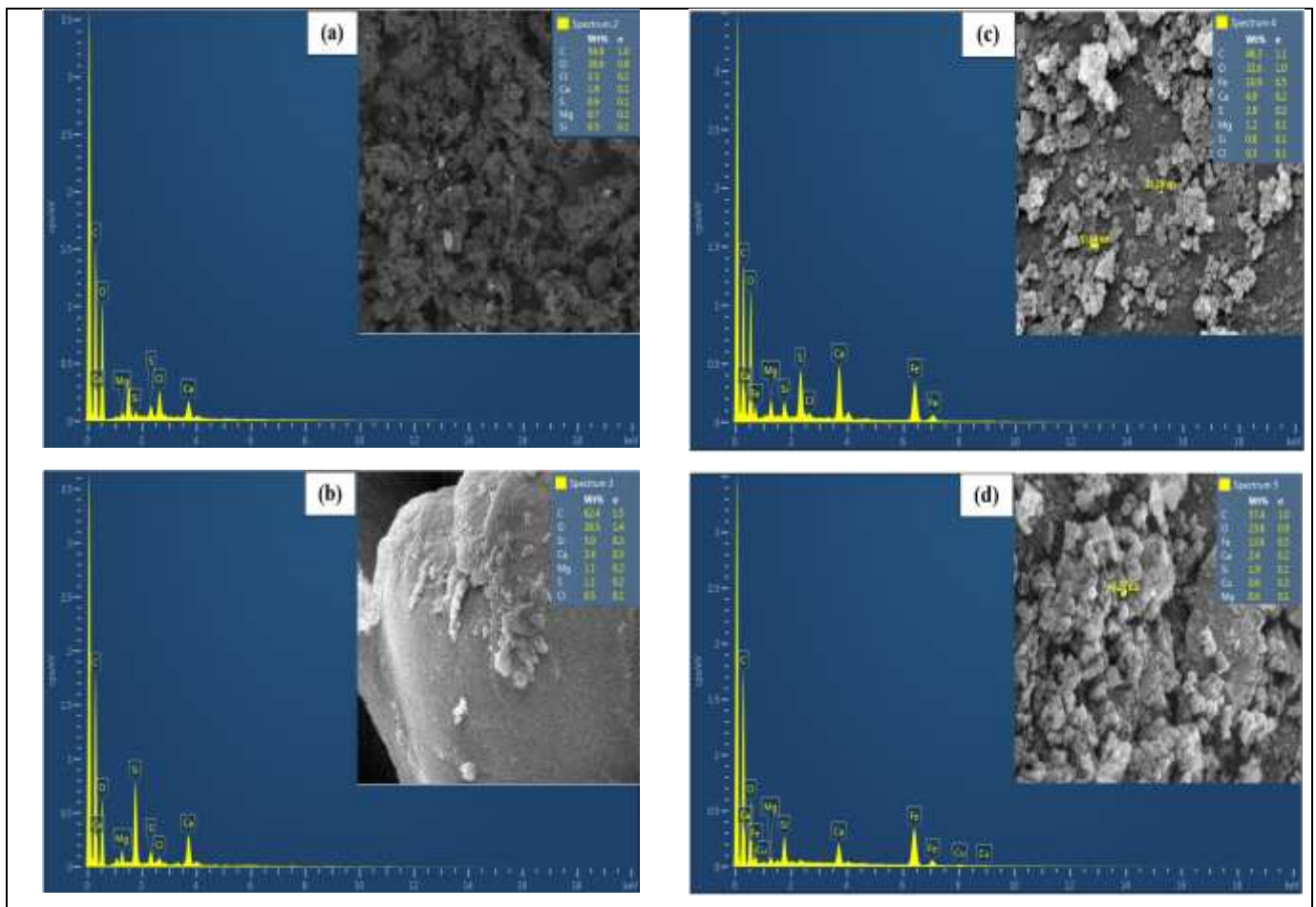


Figure 2. Scanning electron microscopy images and EDS spectrum of (a) LB, (b) AW, (c) AW /MgFe-LDH, and (d) AW/MgFe-LDH after adsorption Copper

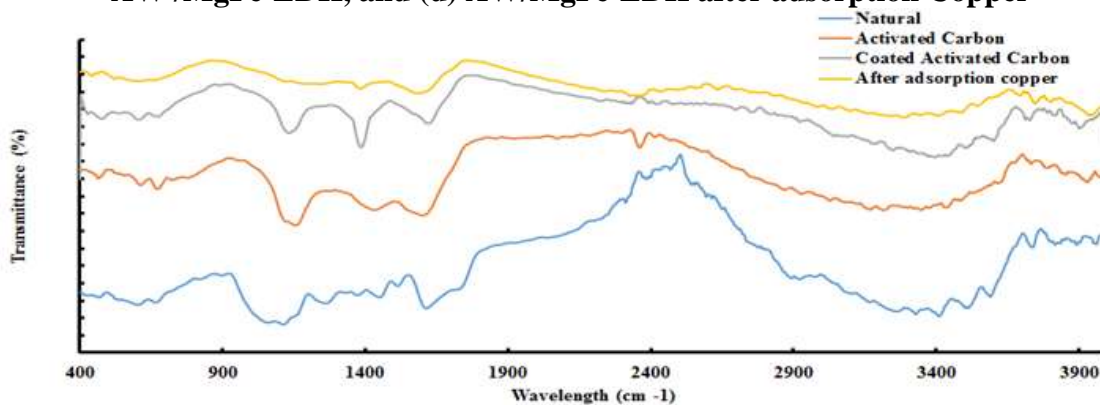


Figure 3. Fourier transform infrared spectra of (a) LB, (b) AW, (c) AW /MgFe-LDH, and (d) AW/MgFe-LDH after adsorption Copper

After adsorption, moving or changing of groups negatively charged peaked in intensity and indicated that they were involved in the adsorption process. According to the increase in the adsorbent surface area from 0.8645 m².g⁻¹ for the LB to 24.5 m².g⁻¹ for the AW and then to the 79.7 m².g⁻¹ for AW/Mg/Fe-LDH, the AW adsorption capacity was improved after several modification processes which ended by coating with Mg/Fe-LDH to

produce a good AW/Mg/Fe-LDH adsorbent for copper.

Effect of amount of elements that synthesized the adsorbent

The first step in synthesizing the AW/Mg/Fe-LDH was to investigate the copper removal at different molar ratios (Mg/Fe), and to analyse how they affect the removal, which is obvious from (Fig. 4 (A)). The copper adsorption capacity on AW was 8.2 mg/g, which was lower compared to the adsorption on Mg/Fe-

LDH (12.4 mg/g) at a 3 molar ratio (Mg/Fe). Therefore, improvement of the adsorption capacity was due to the increase of the Mg amount than the Fe amount. Though, this molar ratio was chosen to compose the adsorbent in order to achieve high adsorption capacities. In addition, the AW content for synthesizing AW/Mg/Fe–LDH with a 3 Mg/Fe molar ratio was examined with different dosages that increase from 0.05 to 0.5 g in a 50 ml solution, and the copper adsorption capacity was improved due to the increase of dosage (Fig. 4 (B)). Thus, it was a dosage of 0.5 g to prepare the AW/Mg/Fe–LDH (Fig. 4 (B)).

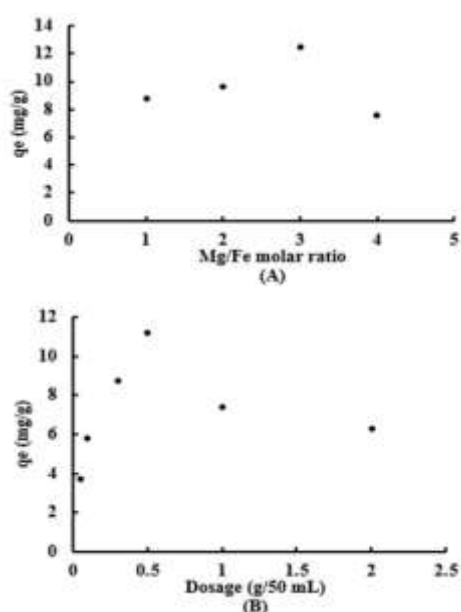


Figure 4. The (A) varying molar ratios Mg/Fe; (B) AW dosage, affecting on Copper sorption capacities (time = 3 hr, pH = 5, and dosage= 0.04 g/50mL)

Equilibrium contact time

For a batch test, the metal removal was investigated by utilizing 0.5 g of the adsorbent with a 50 ml copper solution (Fig. 5). In general, the adsorption process included two stages; first, representing the surface passive reaction, which is a rapid process like chemical or physical sorption; second, indicating the metabolic active reaction, which is slow. It is obvious from Figure 6 that the increased contact time lead to the increase of removed copper percentage, showing that the adsorption was rapid at the primary stage, and after that it gradually slowed down because the number of sorption sites decreased on the AW/Mg/Fe–LDH surface. In 1 hour, the

copper removed reached 96%, but when the contact time was longer than 1 hour up to 2 hours, the metal concentrations remained constant. Therefore, at this contact time other subsequent sorption experiments were conducted.

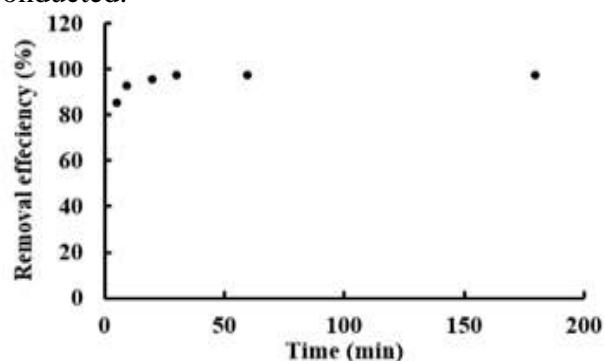


Figure 5. Percentage removal of Copper on adsorbent in different contact time (T= 25±4°C; agitation speed= 200 rpm; dose= 0.5 g/50 ml; C_o=10 mg/l and pH=5).

Variable effect of change initial pH

The pH of solutions affects both contaminant ionic forms, and properties of the surface adsorbent. Therefore, it can be said that the adsorption capacity can be controlled and effected by a primary parameter of pH (Fig. 6) (13,5). The metal adsorption on the sorbent declined at acid state, because the pollutant binding sites were occupied by protons, and on the cell surface most of all reactive sets were protonated (7).

The influence of pollutant initial concentration

By the experimental work, the influence of numerous initial copper concentrations, which adsorbed on the adsorbent, were investigated. The tests were carried with a solution where the pH is equal to 5, with 200 rpm shaking of adsorbent weighting 0.5 g per 100 mL of solution for 1 hour and initial metal concentrations ranging from 10 to 1000 mg/L. The relation between initial copper concentration and metal removal efficiency at equilibrium state are shown in (Fig. 7). At the initial primary values concentration, the higher copper removal was obvious. Cu²⁺ was unable to interact with the samples of reactive media because the available active sites had been saturated. This lead to a gradual decrease of the metal removal capacity at the moment when the initial metal concentration increased. Depending on above stated, as pollutant

concentrations increase, the active sites become less available (9).

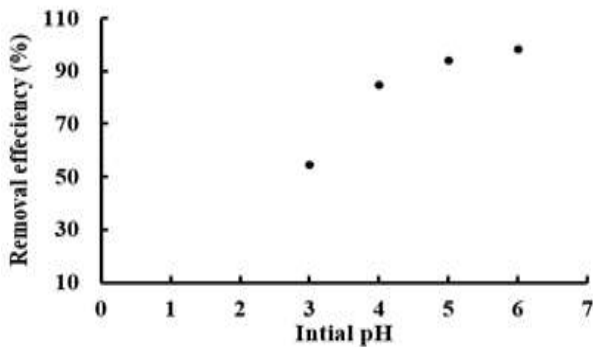


Figure 6. The influence of pH solution on Copper removal efficiency by adsorption on adsorbent (agitation speed= 200 rpm; T= 25±4°C; time=1hr, C_o= 10 mg/l; and dose= 0.1 g/100 mL).

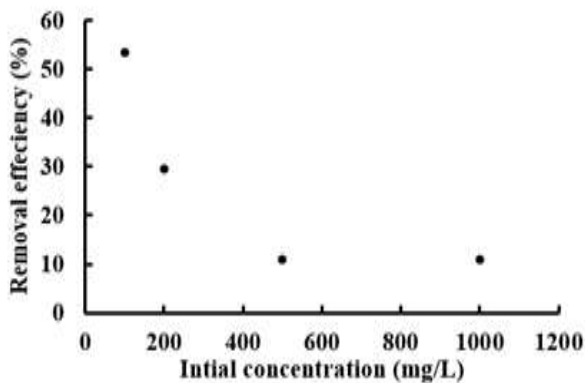


Figure 7. The influence of Copper initial concentration on metal removal efficiency by adsorption on adsorbent (agitation speed= 200 rpm; T= 25±4°C; time=1hr, pH=5; and dose= 0.1 g/100 mL

The influence of initial adsorbent dosage

For batch tests at 25 ± 4 °C, initial adsorbent dosages effecting the copper adsorption on AW/Mg/Fe–LDH were investigated with numerous volumes of the sorbent (0.02 to 0.3 g) in 50 ml copper solution. The relation between amounts of reactive material and metal removal efficiency at equilibrium state are shown in Figure 8. In addition, fixing the initial metal concentration and increasing the adsorbent dosage from 0.02 to 0.3 g/50 mL, the metal removal efficiency improved. When the adsorbent dosage reached 0.2 g, the maximum removal was achieved, and despite increasing the adsorbent dosage, the copper contained in the solution and on the sorbent remained constant.

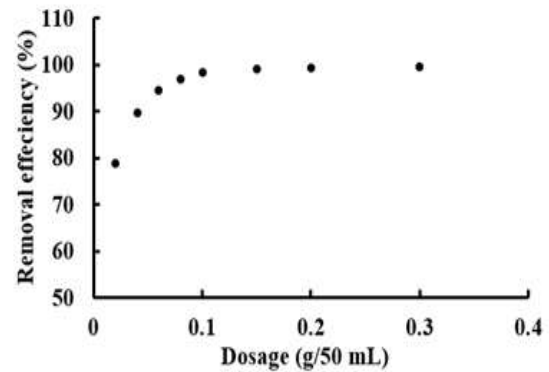


Figure 8. The influence of sorbent dosage on metal removal efficiency by adsorption on adsorbent (agitation speed= 200 rpm; T= 25±4°C; time=1hr, pH=5; and C_o=10 mg/L) **Adsorption isotherms & kinetics**

The experimental data were fattened by isotherms (Langmuir model, Freundlich model) that were presented in (eq. 2) (6) and (eq. 3) (29), respectively. The results shown in Table 1 represent the determination coefficient, parameters and sum square error for the copper sorption on the adsorbent, and they were compared to each isotherm. As a result, it can be seen from this comparison that the Freundlich model (highest R² and lower SSE) was good for the adsorption process.

$$q_e = \frac{q_m b C_e}{1 + b C_e} \tag{2}$$

$$q_e = K_F C_e^{1/n} \tag{3}$$

Where *b* is the constant associated to the free energy adsorption, *q_m* is the maximum adsorption capacity, *C_e* is the solute concentration at equilibrium in the bulk solution (mg/L), *q_e* is the amount of a solute adsorbed per unit weight of an adsorbent at equilibrium (mg/g), *K_F* is the coefficient of Freundlich sorption ((mg/g)(l/mg)^{1/n}) and *n* is an empirical coefficient indicative of the intensity of the adsorption. The pseudo-first-order (eq. 4) (20) and pseudo-second-order (eq. 5) (14) were utilized to study the copper controlling mechanism on the adsorption process for experimental data like a chemical reaction on the sorbent.

$$q_t = q_e (1 - e^{-k_1 t}) \tag{4}$$

$$\frac{t}{q_t} = \left(\frac{1}{k_2 q_e^2} + \frac{t}{q_e} \right) \tag{5}$$

Where *k₁* and *k₂* represent the pseudo-first-order and pseudo-second-order of equilibrium adsorption at a constant rate (L/min), respectively, *q_t* and *q_e* are the quantities of a

sorbate removed from an aqueous solution at time t . The investigation of kinetic models nonlinear forms was done by nonlinear regression analysis (Figure 9).

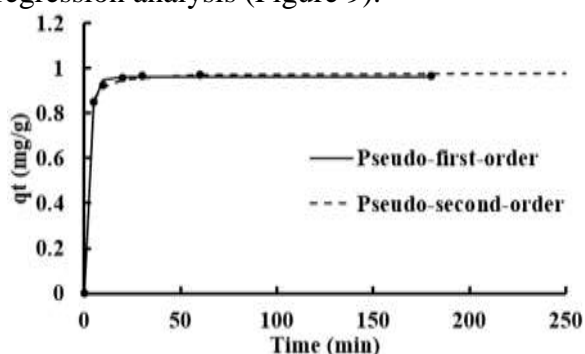


Fig. 9. The applying of Copper nonlinear regression analysis to calculate adsorption kinetics models (agitation speed= 200 rpm; T= 25±4°C; time=1hr, pH=5; and $C_0=10$ mg/L and 0.5 g/50 mL)

The rate of pseudo-first-order and pseudo-second-order for the copper adsorption on AW/Mg/Fe-LDH remained constant, and the

Table 1. The results of sorption isotherm models, pseudo-first-order, and the pseudo-second-order for Copper adsorption (agitation speed= 200 rpm; T= 25±4°C; time=1hr, pH=5; and $C_0=10$ mg/l and 0.5 g/50 mL).

	Models type	Calculated parameters	Cu ⁺²
Isotherm models	Langmuir	q_m	35.39
		b	0.55
		R^2	0.98
		SSE*	7.95
	Freundlich	K_F	12.02
		n	1.62
		R^2	0.99
		SSE*	2.77
kinetics models	Pseudo-first-order	k_1	0.4221
		q_e	0.9596
		R^2	0.9399
		SSE*	0.0007
	Pseudo-second-order	k_2	1.4014
		q_e	0.9816
		R^2	0.9994
		SSE*	0.0005
		q_e exp.	0.965

The novel adsorbent was prepared by simple co-precipitation method including coating the activated carbon derived from agriculture waste, namely leaf base date palm, by Mg/Fe layered double hydroxides. The sorption process was examined for the copper removal from wastewater. The model of Langmuir isotherm and the pseudo-second-order kinetics complied with the copper sorption process according to the kinetics and isotherms studies. In this way, the AW/Mg/Fe-LDH can

values of calculation and experimental q_e are presented in (Table 2). The results show that if the kinetic models apply for the copper sorption, the correlation coefficients (R^2) were higher than 0.99 and the determination sorption capacities were near to the experimental data for the pseudo-second-order, while for the pseudo-first-order, the correlation coefficients (R^2) were very low. However, the kinetic model of the pseudo-second-order complied with the copper sorption process, where chemisorption was suggested. The ion exchange obeys the mechanisms of the copper removal. It is obvious from Figure 3, as copper exchanges with carbonate instead of adsorbing it, the bands at 1375 cm^{-1} changed. The adsorption process involved the negatively charged peaks for moving and changing groups in intensity after the sorption.

be considered to be appropriate copper scavengers with a highly effective Cu²⁺ removal from wastewater

REFERENCES

1. Abdulkareem, H.N. and A. I. Alwared, 2019. Immobilization dried mix of algae for copper removal. Iraqi Journal of Agricultural Sciences, 50(3):800- 808
2. Ahmed, M. J., and S. K. Theydan, 2012. Physical and chemical characteristics of activated carbon prepared by pyrolysis of

- chemically treated date stones and its ability to adsorb organics. *Powder Technology*, 229: 237–245
3. Al-Hassoon, S. N.H.; A.S. J. Z. Al-Hayani, and M. A. J. Al-Obaidi, 2019. Copper adsorption in two different soil texture. *Iraqi Journal of Agricultural Sciences*, 50(2):638-645
 4. Ali, A. H. 2019. Removal of Sulfamethoxazole, Sulfapyridine and Carbamazepine, from Simulated Wastewater Using Conventional and Nonconventional Adsorbents. *International Journal of Environmental Research*, 13 (3): 487–497
 5. Alkan, M.; B.; Kalay, M. Doğan, and Ö. Demirbaş, 2008. Removal of copper ions from aqueous solutions by kaolinite and batch design. *Hazard Mater*, 153 (1-2): 867–876
 6. Allen, S. J.; G. McKay, and J. Porter, 2004. Adsorption isotherm models for basic dye adsorption by peat in single and binary component systems. *Colloid Interface Sci.* 280 (2): 322–333
 7. Areco, M. M.; S.; Hanela, J.; Duran, M. Afonso, and D. Santos, 2012. Biosorption of Cu(II), Zn(II), Cd(II) and Pb(II) by dead biomasses of green alga *Ulva lactuca* and the development of a sustainable matrix for adsorption implementation. *J Hazard Mater*, 213–214: 123–132
 8. Ayawei, N.; A. T.; Ekubo, D. Wankasi, and E. D. Dikio, 2015. Synthesis and Application of Layered Double Hydroxide for the removal of Synthesis and Application of Layered Double Hydroxide for the removal of Copper in Wastewater. *International Journal of Chemistry*, 7 (1): 122–132
 9. Buasri, A.; P.; Yongbut, N. Chaiyut, and K. Phattarasirichot, 2008. Adsorption Equilibrium of Zinc Ions from Aqueous Solution by Using Modified Clinoptilolite. *Chiang Mai J Sci.* 35 (1): 56–62
 10. Facui, Y.; S.; Shiqi, C.; Xiaoqi, C.; Yue, Z. Fei, and L. Ziqiang, 2016. Mg–Al layered double hydroxides modified clay adsorbents for efficient removal of Pb²⁺, Cu²⁺ and Ni²⁺ from water. *Applied Clay Science*, 123: 134–140
 11. Faisal, A. A. H., and L. A. Naji, 2019. Simulation of Ammonia Nitrogen Removal from Simulated Wastewater by Sorption onto Waste Foundry Sand Using Artificial Neural Network. *Association of Arab Universities Journal of Engineering Sciences*, 26 (1): 28–34.
 12. Fu, F., and Q. Wang, 2011. Removal of heavy metal ions from wastewaters: A review. *Journal of Environmental Management*, 92 (3): 407–418
 13. Garg, U. K.; M. P.; Kaur, V. K. Garg, and D. Sud, 2007. Removal of hexavalent chromium from aqueous solution by agricultural waste biomass. *J Hazard Mater. Hazard Mater*, 140 (1-2): 60-68
 14. Goncharuk, V. V.; L. N.; Puzyrnaya, G. N.; Pshinko, A. A. Kosorukov, and V. Y. Demchenko, 2011. Removal of Cu(II), Ni(II), and Co(II) from aqueous solutions using layered double hydroxide intercalated with EDTA. *Journal of Water Chemistry and Technology*, 33 (5): 288–292
 15. Gunatilake, S. K. 2015. Methods of Removing Heavy Metals from Industrial Wastewater. *Journal of Multidisciplinary Engineering Science Studies (JMESS)*, 1 (1): 12–16
 16. Ho, Y. S. and G. McKay, 1999. Pseudo-second order model for sorption processes. *Process Biochemistry* 34 (5): 451–465
 17. Hussein, S. I. 2019. Efficiency of immobilized polyphenol oxidase on some textile dyes degradation using batch operation system by packed bed bioreactor. *Iraqi Journal of Agricultural Sciences*, 50(3):943- 950
 18. Jia Y.; Y. Zhang and J. Fu 2019. A novel magnetic biochar/MgFe-layered double hydroxides composite removing Pb²⁺ from aqueous solution: Isotherms, kinetics and thermodynamics. *Colloids and Surfaces A: Physicochemical and Engineering Aspects*, 567: 278–287.
 19. Khadhri, N.; M. E. K.; Saad, M. Mosbah, and Y. Moussaoui, 2018. Batch and continuous column adsorption of indigo carmine onto activated carbon derived from date palm petiole. *Journal of Environmental Chemical Engineering*, 7 (1): <https://doi.org/10.1016/j.jece.2018.11.020>
 20. Lagergren, S. 1989. About the theory of so-called adsorption of soluble substances. *Kung Seventeen Hand* 24 (4): 1–39
 21. Lewinsk, A. A. 2007. *Hazardous Materials and Wastewater: Treatment, Removal and Analysis*. Nova Publishers, New York. pp: 375

22. Li, S.; Guo, Y.; Xiao, M.; Zhang, T.; Yao, S.; Zang, S. and Y. Shen, 2019. Enhanced arsenate removal from aqueous solution by Mn-doped MgAl-layered double hydroxides. *Environ Sci. Pollu. Res.*, 26 (12): 12014-12024
23. Liang, X.; Y.; Zang, Y.; Xu, X.; Tan, W.; Hou, L. Wang, and Y. Sun, 2013. Sorption of metal cations on layered double hydroxides. *Colloids and Surfaces A: Physicochemical and Engineering Aspects*, 433: 122–131.
24. Murdock, J. N., and D. L. Wetzel, 2009. FT-IR Microspectroscopy Enhances Biological and Ecological Analysis of Algae. *Applied Spectroscopy Reviews*, 44 (4): 335–361
25. Najjah, S.; M.; Yusoff, A.; Kamari, W. P.; Putra, C. F.; Ishak, A. Mohamed, and I. Isa, 2014. Removal of Cu (II), Pb (II) and Zn (II) Ions from Aqueous Solutions Using Selected Agricultural Wastes: Adsorption and Characterisation Studies. *Journal of Environmental Protection*, 5 (4): 289–300
26. Resmije Imeri; Endrit Kullaj; Edmond Duhani and Lulzim Millaku. 2019. Concentration of heavy metals of in apple fruits around the industrial area of Mitrovica, Kosovo. *Iraqi Journal of Agricultural Sciences*, 50(1):256-266
27. Rojas, R. 2016. Effect of particle size on copper removal by layered double hydroxides. *Chemical Engineering Journal*, 303: 331–337
28. Sadon, F. N.; A. S., Ibrahim, and K. N. Ismail, 2014. Comparative Study of Single and Multi-layered Fixed Bed Columns for the Removal of Multi-metal Element using Rice Husk Adsorbents. *Applied Sci.*, 14 (12): 1234–1243.
29. Saha, T. K. 2010. Adsorption of Methyl Orange onto Chitosan from Aqueous Solution. *Water Resource and Protection*, 2 (10): 898–906
30. Sarma, P. J.; R.; Kumar, and K. Pakshirajan, 2015. Batch and Continuous Removal of Copper and Lead from Aqueous Solution using Cheaply Available Agricultural Waste Materials. *Int. J. Environ. Res.*, 9 (2):635–648
31. Sulaymon, A. H., and S. E. Ebrahim, 2008. Increasing the adsorption surface of activated carbon. *Journal of Engineering*, 14 (3): 2700–2717
32. Sultan, M. S.; M. Z.; Thani, H. S. Khalaf, and A. J. Salim, 2018. Determination of some heavy metals in solid waste from heavy water treatment station in Baghdad. *Iraqi Journal of Agricultural Sciences*, 49(3):500-505
33. Tran, H. N.; C. C.; Lin, S. H. Woo, and H. P. Chao, 2018. Efficient removal of copper and lead by Mg/Al layered double hydroxides intercalated with organic acid anions: Adsorption kinetics, isotherms, and thermodynamics. *Applied Clay Science*, 154: 17–27
34. Wang C.; H. Wang and G. Gu 2018. Ultrasound-assisted xanthation of cellulose from lignocellulosic biomass optimized by response surface methodology for Pb(II) sorption. *Carbohydrate Polymers*, 182: 21–28
35. Wang, J., and C. Chen, 2009. Biosorbents for heavy metals removal and their future. *Biotechnology Advances*, 27 (2): 195–226
36. Xie, Y.; X.; Yuan, Z.; Wu, G.; Zeng, L.; Jiang, X. Peng, and H. Li, 2019. Adsorption behavior and mechanism of Mg/Fe layered double hydroxide with Fe₃O₄-carbon spheres on the removal of Pb(II) and Cu(II). *Journal of Colloid and Interface Science*, 536: 440-455.